Experimental estimation of tearing mode stability parameters (Δ' and w_c) using high resolution 2D ECEI data in the KSTAR plasmas

M. J. Choi[1], G. S. Yun[1], W. Lee[2], H. K. Park[2], Y.-S. Park[3], S. A. Sabbagh[3], K. J. Gibson[4], C. Bowman[4], C. W. Domier[5], N. C. Luhmann, Jr.[5], J.-G. Bak[6], S. G. Lee[6] and KSTAR Team[6]

[1] *Pohang University of Science and Technology, Pohang, Gyeongbuk 790-784 Korea*

[2] *Ulsan National Institute of Science and Technology, Ulju-gun, Ulsan 689-798 Korea*

[3] *Department of Applied Physics, Columbia University, New York, NY 10027, USA*

[4] *York Plasma Institute, Department of Physics, University of York, YO10 5DD, UK*

[5] *University of California, Davis, CA 95616, USA*

[6] *National Fusion Research Institute, Daejeon 169-148, Korea*

Evolution of tearing mode instability should be controlled thoroughly for the steady state high performance operation of fusion plasma. For the efficient control of the mode, the accurate estimation of the tearing mode stability parameters and correct understanding of driving/decaying mechanism are important.

After the onset of the instability, the magnetic island size of tearing mode is mainly affected by two dominant terms in the modified Rutherford equation describing the island size evolution [1]. The one is the contribution from the equilibrium current gradient described with the nonlinear classical stability index defined as $\Delta' = \frac{\psi'}{\psi}\Big|_{r_s-w}^{r_s+w}$ where ψ is the helical magnetic flux function, r_s is the minor radius at the rational flux surface and w is the island half-width. The other is the neoclassical drive from the bootstrap current loss inside the island of the flat pressure profile. The critical width for the island pressure flattening is derived as $w_c = \sqrt{\frac{RqL_q}{m}}\left(\frac{\kappa_\perp}{\kappa_\parallel}\right)^{1/4}$ where R is the major radius, q is the safety factor, $L_q = q/(\mathrm{d}q/\mathrm{d}r)$, m is poloidal mode number, $\kappa_\perp$ is the perpendicular heat conductivity and $\kappa_\parallel$ the parallel heat conductivity [2].

The two tearing mode stability parameters Δ' and w_c can be estimated by comparing the measured T_e structure near the magnetic island with the modeled T_e profile [3–5]. The electron temperature profile near the magnetic island of tearing mode can be obtained by solving the heat flow equation. The heat flow $q = -\kappa_\parallel \nabla_\parallel T_e - \kappa_\perp \nabla_\perp T_e$ will have zero divergence without the heat source or sink.

$$\kappa_\parallel \nabla_\parallel^2 T_e + \kappa_\perp \nabla_\perp^2 T_e = 0 \qquad (1)$$

The gradient along the magnetic field can be derived with the helical magnetic flux notation of the magnetic field, i.e. $B = \nabla\psi \times \hat{e}_\phi$ where ψ is the helical magnetic flux function and $\hat{e}_\phi$ is unit vector along the magnetic field at r_s. The equilibrium helical flux function has taken the form of $\psi_0(r) = \frac{\mu_0 I_0}{8\pi}\left(\left(\frac{r}{a}\right)^2 - \left(\frac{r_s}{a}\right)^2\right)^2$ from the parabolic current

profile assumption where I_0 is the peak value of plasma current profile [4]. The perturbed flux function is modeled with three dimensionless parameters α, β, and γ following [4]

$$\begin{aligned} \psi_1(r) &= \frac{\mu_0 I_0}{8\pi}\alpha\left(\frac{r}{r_s}\right)^m\left(1-\beta\frac{r}{r_s}\right) \qquad \text{for } r \le r_s \\ &= \frac{\mu_0 I_0}{8\pi}\left(\frac{\alpha(1-\beta)-\gamma+\gamma r/r_s}{(r/r_s)^{m+1}}\right) \quad \text{for } r > r_s \end{aligned} \tag{2}$$

The above model function of ψ_1 describes various shapes of the perturbed flux better compared to the other models [3, 5] and converges to zero in the both limits $r \to 0$ and $r \to \infty$. Solving equation (1) with (2) and the helical coordinates (r, ζ, ϕ) where the helical angle is $\zeta = m\theta - nz/R_0$ provides the electron temperature profiles $T_e(r, \zeta)$ which depends on four parameters α, β, γ, and $\kappa_\perp/\kappa_\parallel$. First three parameters are related to the magnetic geometry and used to determine Δ', and the conductivity ratio affects the gradient of T_e profile inside the island and decides the critical width w_c.

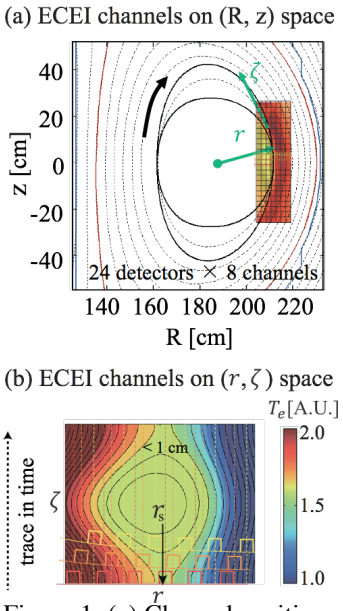

Figure 1: (a) Channel positions of the KSTAR ECEI diagnostic on (R, z) space. Plasma rotates in time and different parts of the magnetic island (illustrated as black line) are captured by the ECEI channels. (b) Translated channel positions on (r, ζ) space. The effective resolution in the r direction is improved significantly.

There have been many attempts to estimate tearing mode parameters Δ' and w_c by comparison between the modeled and measured T_e profiles [3—5]. However, the estimation accuracy was limited to the uncertainty originated from the insufficient spatial resolution of the measured 1D T_e profiles.

The spatial resolution of T_e structure measurement can be greatly improved by adopting 2D diagnostic such as the KSTAR ECEI diagnostic shown in figure 1 [6]. In contrast to the conventional 1D diagnostic, the additional detectors located at different vertical positions increase the effective spatial resolution in (r, ζ) space significantly and fine T_e structure near the island was measured on the KSTAR plasma # 7131.

The core of the KSTAR plasma # 7131 was heated by two NBIs with total power of 3 MW and one 170 GHz ECRH with power of 0.3 MW. The $m/n = 2/1$ magnetic island of the tearing mode was observed around $r/a \approx 0.6$. The magnetic island is far from the core or the edge and the equation (1) is satisfied. In order to estimate Δ' and w_c of the observed tearing mode, the ECE images (figure 2(a)) have been measured and the equation (1) solved near the $2/1$ magnetic island obtained.

For the direct comparison with the measured ECE images, the modeled solution of the heat flow equation ($T_e(r, \zeta; \alpha, \beta, \gamma, \kappa_\perp/\kappa_\parallel)$) is converted into the synthetic ECE images . The instrumental response function of the ECEI channel is applied on the model T_e profiles to get synthetic ECE intensity profiles. The synthetic ECE images are reconstructed by normalization of the synthetic ECE intensity profiles against the time averaged values. Figure

2(b) shows example of the synthetic ECE images reconstructed with the parameter set $\mathbf{p} = [\alpha = 0.0382,\ \beta = 0.949,\ \gamma = -0.00382,\ (\kappa_\perp/\kappa_\parallel)^{1/4}\sqrt{B_0} = 0.00691]$ at four different time points. B_0 is the magnetic field strength at the major radius $R = 1.8$ m.

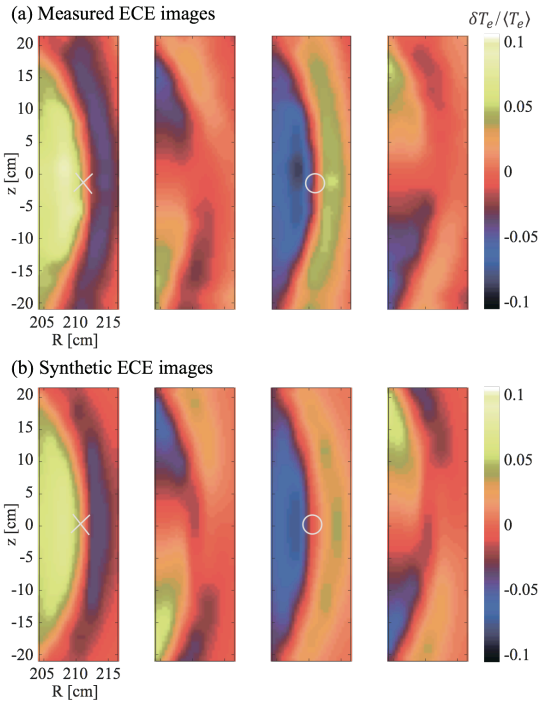

Figure 2: (a) Measured ECE images of the magnetic island at four different time points as it rotates in clockwise direction. X and O marks represent the X- and O-point of the magnetic island, respectively. (b) Synthetic ECE images reconstructed from the model.

For a given parameter set $\mathbf{p}$, $\chi^2(\mathbf{p}) = \frac{1}{2}\sum_{n=1}^{N}[y_n - \hat{y}_n(\mathbf{p})]^2$ is calculated to assess the difference between the measured and synthetic ECE images. N is total number of data points used ($560 = 4$ images $\times$ 140 pixels per image), y_n is the measured ECE image data and $\hat{y}_n(\mathbf{p})$ the synthetic ECE image data of $\mathbf{p}$.

Finding the χ^2 minimum is non-trivial because the model has multi parameters and the Levenberg-Marquardt algorithm was applied. This algorithm updates the randomly given parameter values toward the minimal point of χ^2 using the gradient descent method and Gauss-Newton method.

The result of the parameter searching for the minimum χ^2 is shown in figure 3. The global minimum of χ^2 is achieved as 0.0402 at $\alpha = 0.0382$, $\beta = 0.949$, $\gamma = -0.00382$ and $(\kappa_\perp/\kappa_\parallel)^{1/4}\sqrt{B_0} = 0.00691$. Because χ^2 includes the measurement error of the ECEI data ($\sqrt{((\partial\chi^2/\partial y)\delta y)^2} \approx 0.002$), the group of parameter sets of $\chi^2 < 0.0422$ (below the dashed line in figure 3) are selected for Δ' and w_c estimation.

Using the selected parameter sets, $\Delta' = \frac{\psi'}{\psi}\Big|_{r_s-w}^{r_s+w}$ and $w_c = \sqrt{\frac{RqL_q}{m}}\left(\frac{\kappa_\perp}{\kappa_\parallel}\right)^{1/4}$ are calculated. The island half-width w is estimated as 3 cm from the measured ECE images. The result of Δ' and w_c calculations is fitted into the Gaussian function, and $r_s\Delta' = -1.633 \pm 1.265$ and $w_c = 0.612 \pm 0.0726$ cm are obtained. These values mean that the observed tearing mode is classically stable (negative Δ') but the neoclassical drive from the bootstrap current loss is non-negligible ($w_c/w \sim 0.2$).

The accurate estimation of Δ' and w_c with the reasonable error was possible due to high resolution data of the KSTAR ECEI diagnostic. It enhanced the resolving power between the T_e models over four parameter spaces and allowed high confidence in the selected parameter sets. The Δ' estimation result could be compared with the prediction from the ideal MHD calculation. The tearing mode equation of ψ_1 was integrated with the shooting method [7] and the ideal $r_s\Delta'_{ideal} = -4.12$ has the same negative sign.

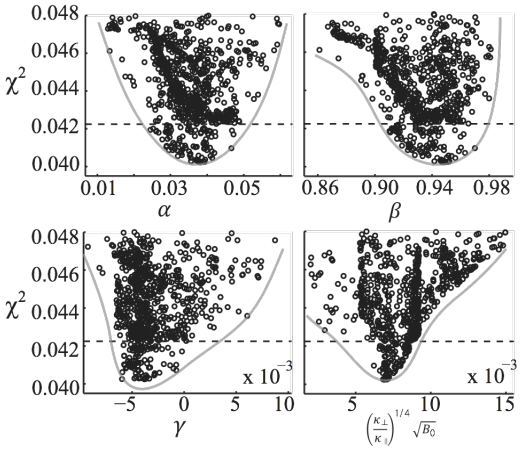

Figure 3: Distribution of χ^2 local minimal points is shown. The global minimum point is found over four dimensional parameter space.

In summary, high spatial resolution 2D images of T_e fluctuations near the $2/1$ magnetic island have been measured with the KSTAR ECEI diagnostic, and two important tearing mode parameters Δ' and w_c were estimated accurately. The tearing mode is analyzed to be classically stable, but to have finite neoclassical bootstrap current drive. The Δ' and w_c estimation method developed in this paper can be applied over long evolution period of tearing mode and growth/decay of the mode will be analyzed based on the modified Rutherford equation and the measured tearing mode parameters.

[1] H. R. Wilson, *Fusion Sci. Technol.* **45** 123–31 (2004)
[2] R. Fitzpatrick, *Phys. Plasmas* **2** 825–38 (1995)
[3] C. Ren et al., *Phys. Plasmas* **5** 450–4 (1998)
[4] J. P. Meskat et al., *Plasma Phys. Control. Fusion* **43** 1325–32 (2001)
[5] J. A. Snape et al., *Plasma Phys. Control. Fusion* **54** 085001 (2012)
[6] G. S. Yun et al., *Rev. Sci. Instrum.* **81** 10D930 (2010)
[7] Y. Nishimura et al., *Phys. Plasmas* **5** 4292–9 (1998)